Photoionization of vibrationally excited molecular hydrogen*

H. Tai and M. R. Flannery
School of Physics, Georgia Institute of Technology, Atlanta, Georgia 30332
(Received 25 February 1977)

Cross sections for the photoionization of $H_2(X\,^1\Sigma_g^+, v_i)$ in vibrational levels $v_i = 0$–14 are determined for a range of photon energies by a two-center treatment in which the derived electronic matrix elements are averaged over the initial and final vibrational states of the molecule and the molecular ion. Very good agreement with available measurements for $v_i = 0$ is obtained. Cross sections for the full Franck-Condon array of accessible transitions $H_2(v_i) \rightarrow H_2^+(v_f)$ are also presented. In the energy range considered, when the $2p\sigma_u$ dissociative state of H_2^+ is inaccessible, substantial contributions (up to 50% for $v_i = 6$–10) to the photoionization originate from H^+ atomic ions which are formed via transitions to the vibrational continuum associated with the $1s\sigma_g$ state of H_2^+. Single-center and fixed-nuclei approximations which permit great simplification to the present treatment are also fully investigated.

I. INTRODUCTION

The advent of new techniques in photoelectron spectroscopy[1] and feasibility studies of excimer and rare-gas–halide laser systems have stimulated renewed interest in theoretical descriptions of photoionization, particularly of diatomic molecules. In contrast to photoionization of atoms, for which a central field model permits routine application,[2] relatively little is known theoretically about molecular photoionization, being due in part to the additional complexity introduced by the multicentered nature of the field in which the ejected electron moves. For diatomics, expansion of the continuum wave function in a two-center elliptical basis set facilitates a solution. This approach was adopted for H_2 photoionization by Flannery and Opik,[3] who took account of both the two-center problem and the explicit dependence of the associated electronic transition matrix element with the nuclear separation R. Various modifications to this basic treatment have since been proposed[4,5] as have also various less elaborate descriptions rendered simple by adopting single-center[6–9] and double-center[10] (or deformed) Coulomb waves and fixed-nuclei[6,9] approximations. All of these simplifications have realized varying degrees of success. Also, theoretical attention has focused primarily on the photoionization of molecules initially in the ground vibrational and electronic state, and little has been achieved for molecular systems initially in vibrationally[11,12] and/or electronically excited[13] states.

In this paper, the photoionization process

$$h\nu + H_2(^1\Sigma_g^+, v_i = 0\text{–}14) \rightarrow H_2^+(^2\Sigma_g^+, v_f = 0\text{–}18) + e \qquad (1)$$

is investigated as a function of photon energy $h\nu$ and of the initial and final vibrational levels v_i and v_f of the molecule and molecular ion, respectively, by application of the treatment previously outlined[3] to cases involving a wider range of physical parameters such as the nuclear separation R in H_2, photon frequency $h\nu$ and hence energy ϵ of ejection. Although the $2p\sigma_u$ dissociative state of H_2^+ is inaccesible in the energy range considered, atomic ions H^+ can, however, be formed by direct transitions to the vibrational continuum associated with the $1s\sigma_g$ state of H_2^+. The variation of the associated bound-free Franck-Condon factors[12] with v_i suggests that this mechanism would contribute fairly substantially to the overall photoionization process, particularly for $v_i \sim 6$. This important mechanism for the production of H^+ will therefore be acknowledged theoretically in this study. Finally, in an effort to assess their general utility, various simplified models will be fully explored since the basic inadequacies in both the single-center and fixed-nuclei approximations, normally adopted, are expected to become more apparent as v_i is increased.

II. THEORY

A. Cross section

The cross section for photoionization from a given vibrational and rotational level (v_i, J_i) of the ground electronic state of H_2 to a final level (v_f, J_f) of H_2^+ is given, in the dipole-length formulation, by[3]

$$\sigma_{if}(\nu) = \frac{8\pi^3 e^2 \nu}{3c} \sum_d |\langle \chi_i(\vec{r}, \vec{R}) | \vec{r} | \chi_f(\vec{r}, \vec{R}) \rangle_{\vec{r},\vec{R}}|^2, \qquad (2)$$

where d is the degeneracy of the product $(e\text{-}H_2^+)$ system. According to the Born-Oppenheimer approximation, the wave functions $\chi_{i,f}$ for the neutral H_2 and ionic $(e\text{-}H_2^+)$ molecular systems can be decomposed as the following product:

$$\chi_n(\vec{r},\vec{R}) = (1/R)\psi_n(\vec{r},R)P_n(v_n,J_n;R) \times Y_{J_nM_n}(\hat{R}), \quad n=i,f \tag{3}$$

of their electronic parts $\psi_n(\vec{r},R)$, vibrational parts $P_n(R)$, and rotational (spherical harmonic) parts $Y_{J_nM_n}(\hat{R})$.

The nuclear separation is $\vec{R}$, and $\vec{r}$ denotes the set $(\vec{r}_1,\vec{r}_2)$ of electronic coordinates with respect to a rotating set of axes in which $\vec{R}$ and the center of mass is fixed. The final electronic wave function ψ_f for the $H_2^+ + e$ system contains an implicit dependence on the energy ϵ of the ejected electron given in terms of the energy of transition E_{fi} between the two molecular states and of photon energy $h\nu$ by

$$\epsilon(v_f,J_f;v_i,J_i) = h\nu - E_{fi}(v_f,J_f;v_i,J_i). \tag{4}$$

Assume that the photoionization leaves the molecular rotation unaffected (a good approximation[14]), such that the cross section (2) reduces to

$$\sigma_{if}(\nu,v_i,v_f) = \frac{8\pi^3e^2\nu}{3c}\sum_d \left| \int_0^\infty P_i(v_i,R)\vec{M}_{if}(R,\epsilon) \times P_f(v_f;R)\,dR \right|^2, \tag{5}$$

in which the electronic matrix element vector

$$\vec{M}_{if}(R,\epsilon) = \langle \psi_i(\vec{r},R)\,|\,\vec{r}\,|\,\psi_f(\vec{r},R;\epsilon)\rangle \tag{6}$$

is averaged over the initial and final vibrational wave functions. Noting that the X and Y Cartesian components M_x and M_y of $\vec{M}$ are equal, and that they allow transitions to the (doubly degenerate) final π states of the $H_2^+ + e$ system while the Z component, M_z, permits only σ-σ transitions, then (5) can be written as

$$\sigma_{if}(\nu;v_i,v_f) = \tfrac{4}{3}\pi^2\alpha h\nu[4\,|\langle v_i|M_x|v_f\rangle|^2 + |\langle v_i|M_z|v_f\rangle|^2], \tag{7}$$

$$\alpha = e^2/\hbar c \cong \tfrac{1}{137},$$

where $\langle\ \rangle$ denotes an average over the initial and final vibrational wave functions associated with the rotational level $J_i = J_f$, taken here as zero.

B. Electronic wave functions

A fairly accurate representation of the *initial* electronic $^1\Sigma_g^+$ state of H_2 is the two-parameter Weinbaum function[15]

$$\psi_i(\vec{r},R) = N[\sigma_g(\vec{r}_1)\sigma_g(\vec{r}_2) + c\sigma_u(\vec{r}_1)\sigma_u(\vec{r}_2)], \tag{8}$$

in which the bonding and antibonding molecular orbitals are

$$\sigma_{g,u}(\vec{r}_i) = (Z^3/\pi)^{1/2}(e^{-Zr_{iA}} \pm e^{-Zr_{iB}}), \quad i=1,2, \tag{9}$$

where r_{iA} and r_{iB} are the distances from nuclei A and B, respectively. The parameters c and Z are determined for various values of the internuclear distance R by a variational calculation which minimizes the energy at each R. Flannery[16] has previously obtained these variational parameters for certain selected R in the range $1 \le R(a_0) \le 2$ relevant to ionization of the $v_i = 0$ state. These parameters, required over a more closely spaced mesh of a much wider R range because ionization from all initial states $v_i = 0$–14 are studied, are now determined for the R range $(0.6$–$5)a_0$ and may be obtained from the authors.

The wave function for the *final* electronic state of the $H_2^+ + e$ system is taken, as before, to be

$$\psi(\vec{r},R,\epsilon) = 2^{-1/2}[\psi^+_{1s\sigma_g}(\vec{r}_1,R)F_\epsilon(\vec{r}_2,R) + \psi^+_{1s\sigma_g}(\vec{r}_2,R)F_\epsilon(\vec{r}_1,R)], \tag{10}$$

in which the *exact* electronic ground-state wave function for H_2^+ is separable in elliptic coordinates (λ,μ,ϕ) as

$$\psi^+_{1s\sigma_g}(\vec{r},R) = N^+(R)\Lambda^+_{00}(R;\lambda)M^+_{00}(R;\mu), \tag{11}$$

where the normalization factor N^+ and the functions of λ and μ have been given by Bates *et al.*[17] The continuum orbital to be determined is normalized per unit energy interval, i.e., according as,

$$\langle F_\epsilon(\vec{r})\,|\,F_{\epsilon'}(\vec{r})\rangle = \delta(\epsilon - \epsilon'). \tag{12}$$

The chief contribution to the "dipole-length" matrix element (6) originates from the continuum orbital at fairly large distances from the nuclei. At such distances the $1s\sigma_g$ valence electron provides sufficient screening that the field experienced by the ejected electron may be approximated as that arising from two point charges each of $\frac{1}{2}e$. These fictitious charges are separated by a distance R' chosen so that the associated quadrupole moment is equal to that of the residual $H_2^+(1s\sigma_g)$ ion with nuclear separation R. Thus, it can be shown that

$$R'^2 = 2R^2 + 4\langle\psi^+_{1s\sigma_g}(\vec{r},R)\,|\,x^2 - z^2\,|\,\psi^+_{1s\sigma_g}(\vec{r},R)\rangle_{\vec{r}}. \tag{13}$$

This model is apparently fairly accurate for the small and intermediate values of $R < 5a_0$ relevant here, but is, of course, incorrect in the limit of infinite R, when, coupling with the $2p\sigma_u$ state becomes important such that the electron in H_2^+ is then bound to only one nucleus. Thus within this framework, the continuum orbital F for the ejected electron can now be determined exactly in elliptic coordinates by inserting the product

$$F(R',\epsilon;\lambda,\mu,\phi) = N^e_{lm}\frac{P_{lm}(R',\epsilon;\lambda)}{(\lambda^2-1)^{1/2}}M^e_{lm}(R',\epsilon;\mu)e^{im\phi} \tag{14}$$

into the Schrödinger equation for motion of an electron of mass m_e and energy ϵ under two point

charges ($\frac{1}{2}e$) separated by a distance R' given by (13). It then follows that

$$M^e_{lm}(R', \epsilon; \mu) = \sum_{n=1}^{\infty} f^{lm}_n(p) P^m_{m+n}(\mu) , \tag{15}$$

the prolate spheroidal function, where the coefficients f_n of the associated Legendre functions P^m_{m+n} are tabulated[18] as functions of the indices l, m, separation constant A_{lm} and of the continuous variable

$$p^2 = \tfrac{1}{4}(2m_e\epsilon/\hbar^2)R'^2 \tag{16}$$

The "radial" functions are determined by the numerical integration of

$$\frac{d^2P_{lm}(R', \epsilon)}{d\lambda^2} + \left(\frac{p^2\lambda^2 + (m_e/\hbar^2)2R'\lambda + A_{lm}}{(\lambda^2 - 1)} + \frac{1 - m^2}{(\lambda^2 - 1)^2}\right) P_{lm}(R', \epsilon) = 0 , \tag{17}$$

subject to the asymptotic condition

$$P_{lm}(R', \epsilon; \lambda) \xrightarrow{\text{large } \lambda} \frac{2}{R'}\left(\frac{m_e R'}{\hbar^2 \pi p}\right)^{1/2} \sin(p\lambda + \eta) \tag{18}$$

with phase shift η, and amplitude chosen so as to fulfill the δ-function normalization (12). This normalization may be compared with the one-center atomic case by setting

$$p\lambda \to (2m_e\epsilon/\hbar^2)^{1/2} r \equiv kr .$$

The amplitude of (18) is $2/(\pi p R')^{1/2}$ when ϵ is expressed in atomic units $m_e/\hbar^2 = 1$, and is $(2/\pi p R')^{1/2}$ when ϵ is expressed Rydberg units $2m_e/\hbar^2 = 1$. A more accurate solution for the continuum electron in the field of the H_2^+ ion differs from (18) for two point charges separated by R' by an additional phase $\pi\delta(\epsilon)$, where δ is a quantum defect reflecting the departure of the present model from the actual (e-H_2^+) interaction. This phase can be determined from a suitable extrapolation of quantum defects for the highly excited states of H_2, but, for reasons given previously,[3] it is ignored, although its neglect[3] could involve errors as large as 12%.

The total function F is then fully normalized by setting in (14)

$$N^e_{lm} = \left(2\pi \sum_n f^{lm}_n(p) \frac{2}{2(m+n)+1} \frac{(2m+n)!}{n!}\right)^{-1/2} , \tag{19}$$

where the sum is over even n for $(l - m)$ even, and over odd n for $(l - m)$ odd.

C. Electronic matrix elements

The Cartesian components of the matrix element (6) can be reduced to

$$M_x(R, \epsilon) = M_y(R, \epsilon) = \sqrt{2}\, N^e_{11} d^e_g(\bar{x}) S^+_g \tag{20}$$

for σ_g-π_u transitions ($l = 1$, $m = \pm 1$) and to

$$M_z(R, \epsilon) = \sqrt{2}\, N^e_{10}[d^e_g(\bar{z}) S^+_g + c d^+_u(\bar{z}) S^e_u] \tag{21}$$

for σ_g-σ_u transitions ($l = 1$, $m = 0$). Here the single-electron dipoles are given in terms of the orbitals (9), (11), and (14) for H_2^+ and the continuum electron, as

$$d^e_g(\bar{x}, R) = \int \sigma_g(R) x F(\pi_u, R', \epsilon)\, d\vec{r} , \tag{22}$$

$$d^e_g(\bar{z}, R) = \int \sigma_g(R) z F(\sigma_u, R', \epsilon)\, d\vec{r} , \tag{23}$$

$$d^+_u(\bar{z}, R) = \int \sigma_u(R) z \psi^+_{1s\sigma_g}\, d\vec{r} , \tag{24}$$

and the one-electron overlap integrals are simply

$$S^+_g(R) = \int \sigma_g \psi^+_{1s\sigma_g}\, d\vec{r} , \tag{25}$$

$$S^e_u(R) = \int \sigma_u F(\sigma_u, R', \epsilon)\, d\vec{r} . \tag{26}$$

Both sets of integrals are parametric in R and ϵ.

The second term in the z component (21) is the contribution from indirect transitions arising from the overlap between the ungerade bound and free orbitals with σ_u character. Explicit calculations show that the sign of this term is opposite to that of the first term for all R, and zeros in the matrix element M_z occur for various combinations of R and ϵ (see Fig. 2).

With the aid of (9) and (11) the overlap (25) is

$$S^+_g(R) = 8\pi N^+ \left(\frac{R}{2}\right)^3 \left(\frac{Z^3}{\pi}\right)^{1/2} \int_1^{\infty} \Lambda^+_{00}(R; \lambda) \times \exp(-ZR\lambda/2)(S_0\lambda^2 - S_2)\, d\lambda , \tag{27}$$

where

$$S_n(R) = \sum_{s=0,2}^{\infty} f_s(R) \int_0^1 \mu^n \cosh(ZR\mu/2) P_s(\mu)\, d\mu . \tag{28}$$

Similarly, one can show that

$$S^e_u(R) = 2\pi N^e_{10} \left(\frac{R'}{2}\right)^3 \left(\frac{Z^3}{\pi}\right)^{1/2} \int_1^{\infty} \Lambda^e_{10}(R'; \lambda') \times \int_{-1}^{+1} \left[\exp\left(-\frac{ZR}{2}\beta^+(\lambda', \mu')\right) - \exp\left(-\frac{ZR}{2}\beta^-(\lambda', \mu')\right)\right] \times M^e_{10}(R'; \mu')(\lambda'^2 - \mu'^2)\, d\lambda'\, d\mu' , \tag{29}$$

where $\beta^{\pm}$ which arise from the transformation (13) in (9) are,

$$\beta^{\pm}(\lambda', \mu') = \lambda(\lambda', \mu') \pm \mu(\lambda', \mu') = [\alpha^2(\lambda'^2 + \mu'^2) \pm 2\alpha\lambda'\mu' + (1 - \alpha^2)]^{1/2} , \quad \alpha = R'/R . \tag{30}$$

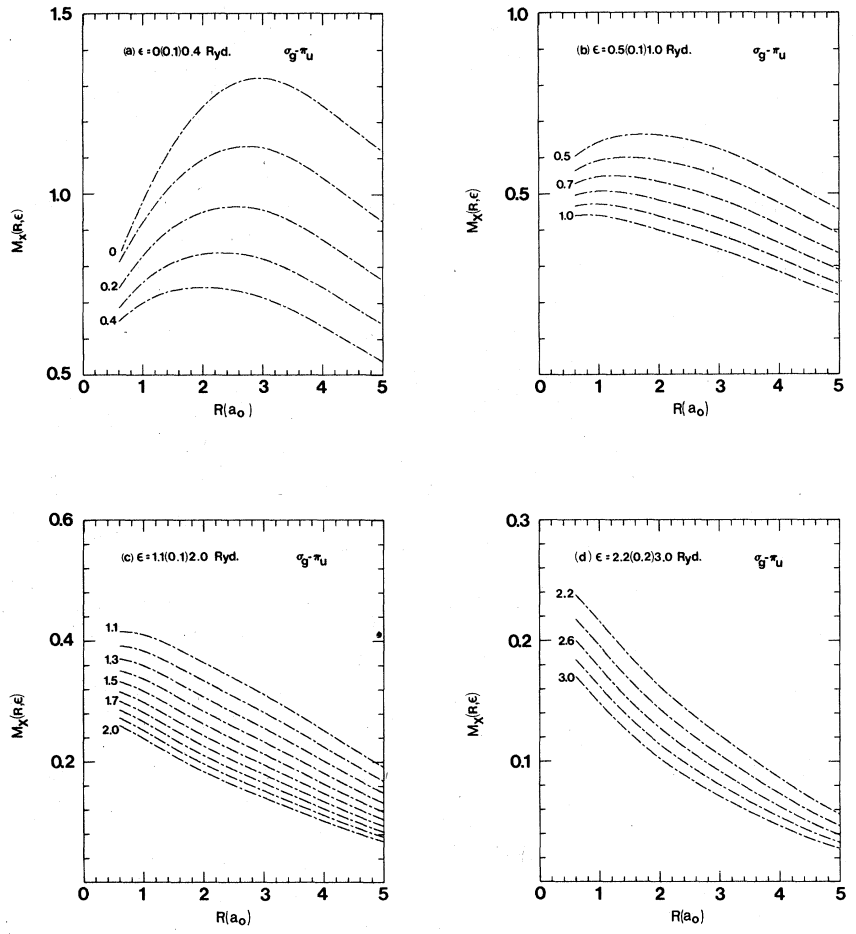

FIG. 1. Variation of the x component of the electronic transition matrix element $\vec{M}_{if}(R,\epsilon)$ with the nuclear separation R of H_2 and with energy ϵ of the ejected electron.

By introducing

$$x = \tfrac{1}{2} R[(\lambda^2 - 1)(1 - \mu^2)]^{1/2} \cos\phi \tag{31}$$

and

$$z = \tfrac{1}{2} R\lambda\mu\,, \tag{32}$$

similar expressions for (22)–(24) can also be written.

By means of a rather lengthy computer program, the components (20) and (21) of $\vec{M}_{if}$ were determined as functions of the internuclear distance R of H_2 and of the energy ϵ of the ejected electron, with R ranging from $0.6a_0$ in steps of $0.2a_0$ to $5a_0$ and with ϵ ranging from 0 in steps of 0.1 Ry (≡1.36 eV) to 3 Ry (≡41 eV). Graphical displays of the resulting M_x and M_z components as functions of R and ϵ are presented in Figs. 1 and 2. In general, both sets of matrix elements M_x and M_z display maxima which progressively flatten, diminish, and shift towards smaller R with increasing ejected energy ϵ [Figs. 1(a), 1(b), 2(a), and 2(b)]. For sufficiently large $\epsilon \gtrsim 1$ Ry, a decrease of M_x and M_z with R and ϵ is, in general, exhibited [Figs. 1(c), 1(d), 2(c), and 2(d)]; however M_z, for large R, increases (becomes less negative) as ϵ is increased. While $M_z > M_x$ in the important range $0.6 < R < R^*$ (where R^* varies from $2.4a_0$ for $\epsilon = 0$ to $1a_0$ for $\epsilon = 3$ Ry), the effective contribution $4|M_x|^2$ in (7) for the σ-π transitions is always greater than $|M_z|^2$, the contribution to the σ-σ probability. Direct calculation shows that the first term in (21) for M_z is always positive while the second term, which originates from the antibonding character of $H_2(X\,^1\Sigma_g^+)$, is always negative such that, as shown in Fig. 2, zeros in $M_z(R,\epsilon)$ appear at specific values R_0 of the internuclear distance. Thus, the σ-σ transition probability vanishes at R_0 which varies from $4.9a_0$ at $\epsilon = 0$ to $2.5a_0$ at $\epsilon = 3$ Ry. This R range is outside the range important to photoionization of the lower-lying vibrational levels of $H_2(X\,^1\Sigma_g^+)$. For higher v_i, the effect of these discrete zeros in M_z is swamped by the rapid oscillations in the vibrational wave functions.

The cross section (7) for photoionization of $H_2(v_i)$ accompanied by a vibrational transition to level v_f of H_2^+ is obtained by averaging both M_x and

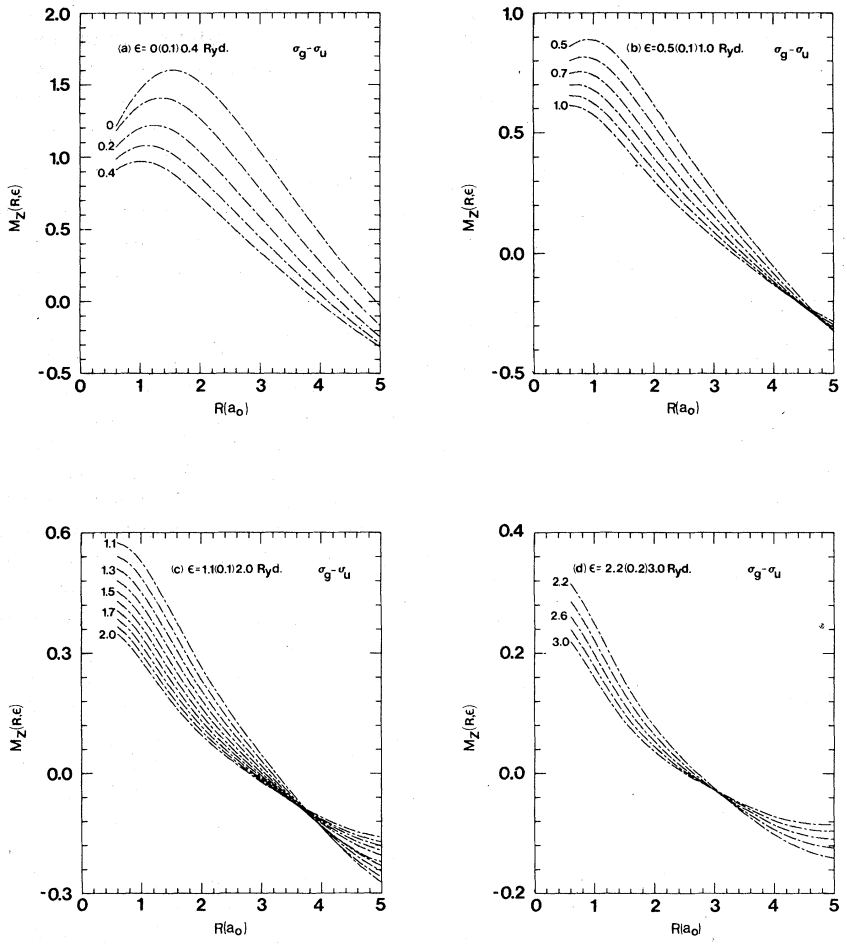

FIG. 2. Variation of the z component of the electronic transition matrix element $\tilde{M}_{if}(R,\epsilon)$ with the nuclear separation R of H_2 and with energy ϵ of the ejected electron.

M_z over the associated initial and final vibrational wave functions. It is therefore convenient to seek a parametric fit to these electronic matrix elements as functions of R and ϵ. The coefficients appearing in the functional form,

$$M_{x,z}(R,\epsilon)=A_{x,z}(\epsilon)+B_{x,z}(\epsilon)[R-R_e]+C_{x,z}(\epsilon)[R-R_e]^2,\quad R_e=1.4a_0, \qquad (33)$$

which reproduced the numerical values of $M_{x,z}$ to well within 1% for various R regions can be obtained from the authors.

D. Vibrational wave functions and moments

All the necessary vibrational wave functions for the $H_2(X\,^1\Sigma_g^+, v_i=0-14, J_i=0)$ and $H_2^+(X\,^2\Sigma_g^+, v_f=0-18, J_f=0)$ systems were obtained by methods previously described.[19] Here, the *ab initio* potentials of Kolos and Wolniewicz[20] for H_2 and the exact diabatic potentials of Hunter *et al.*[21] were adopted in the radial Schrödinger equation solved by the Cooley-Numerov method.[22] Thus, from the determination of the Franck-Condon overlaps $\langle v_i|v_f\rangle$ for the $H_2(v_i)\rightarrow H_2^+(v_f)$ transition and of the two moments $\langle v_i|(R-R_e)^n|v_f\rangle$ for $n=1$ and 2, the cross section (7) for photoionization accompanied by any $v_i\rightarrow v_f$ transitions can be readily evaluated with the aid of (33).

III. CROSS SECTIONS

A. Photoionization from individual vibrationally excited states

Accordingly, we have obtained cross sections $\sigma_{if}(\nu; v_i, v_f)$ for the photoionization processes,

$$h\nu + H_2(X\,^1\Sigma_g^+, v_i=0-14) \rightarrow H_2^+(X\,^2\Sigma_g^+, v_f=0-18)+e \qquad (34)$$

as a function of photon frequency ν and of the initial and final vibrational levels v_i and v_f, respectively, of the neutral molecule and residual molecular ion. A representative display of the results of all possible combinations of v_i and v_f accessible at the wavelength 584 Å (of radiation emitted by the 2^1P-1^1S transition in He) is given in Table I. Similar displays for wavelengths λ from

TABLE I. Cross sections (10^{-18} cm^2) for the photoionization processes, $h\nu + H_2(X^1\Sigma_g^+, v_i) \rightarrow H_2^+(X^2\Sigma_g^+, v_f) + e$ at 584 Å (≡21.2 eV). The cross sections summed over v_f are denoted by Σ.

	V_i														
V_f	0	1	2	3	4	5	6	7	8	9	10	11	12	13	14
0	5.180−1	1.407+0	1.498+0	8.049−1	2.322−1	3.540−2	2.612−3	6.697−5	3.004−6	2.003−6	3.018−6	4.705−7	6.383−8	3.751−7	2.611−7
1	9.676−1	9.324−1	1.685−2	5.540−1	1.045+0	5.732−1	1.309−1	1.148−2	1.568−4	2.613−5	9.808−6	2.189−7	1.470−6	2.603−6	1.407−6
2	1.106+0	2.210−1	3.435−1	5.405−1	5.689−3	6.905−1	8.113−1	2.681−1	2.563−2	2.248−4	2.664−5	3.175−6	1.719−6	7.320−7	2.073−7
3	1.012+0	1.391−4	5.819−1	2.204−2	4.542−1	1.679−1	2.459−1	8.508−1	4.122−1	4.074−2	2.260−4	8.647−5	1.464−5	5.055−8	1.834−6
4	8.209−1	1.020−1	3.844−1	1.175−1	3.164−1	9.181−2	3.873−1	2.501−2	7.630−1	5.343−1	4.533−2	1.269−3	9.045−5	4.310−5	1.055−5
5	6.219−1	2.676−1	1.301−1	3.251−1	3.267−2	3.323−1	9.520−3	3.650−1	1.155−2	6.440−1	6.200−1	3.031−2	6.110−3	3.933−4	3.674−5
6	4.529−1	3.770−1	1.029−2	3.406−1	2.950−2	2.250−1	1.149−1	1.336−1	2.119−1	7.100−2	5.791−1	6.464−1	6.315−3	9.437−3	2.038−3
7	3.228−1	4.125−1	1.192−2	2.266−1	1.510−1	4.851−2	2.386−1	1.200−3	2.215−1	7.945−2	1.067−1	6.215−1	5.440−1	3.970−2	1.619−3
8	2.278−1	3.948−1	6.709−2	1.040−1	2.238−1	1.078−3	1.790−1	9.484−2	4.305−2	1.999−1	1.705−2	8.659−2	8.058−1	2.141−1	9.534−2
9	1.606−1	3.490−1	1.254−1	2.847−2	2.149−1	4.651−2	6.831−2	1.648−1	4.790−3	1.110−1	1.291−1	1.007−3	3.393−2	9.815−1	2.333−2
10	1.134−1	2.934−1	1.647−1	1.395−3	1.608−1	1.032−1	7.815−3	1.425−1	6.207−2	1.632−2	1.265−1	6.921−2	1.599−3	9.752−2	3.757−1
11	8.040−2	2.385−1	1.810−1	4.155−3	1.002−1	1.314−1	2.957−3	8.191−2	1.048−1	3.029−3	5.649−2	9.857−2	3.827−2	3.632−2	3.019−1
12	5.719−2	1.891−1	1.782−1	1.836−2	5.315−2	1.291−1	2.309−2	3.221−2	1.040−1	3.018−2	9.683−3	6.951−2	6.145−2	4.295−2	2.516−1
13	4.068−2	1.468−1	1.621−1	3.222−2	2.379−2	1.086−1	4.313−2	7.090−3	7.827−2	5.301−2	2.581−4	3.113−2	5.476−2	2.923−2	2.276−1
14	2.871−2	1.109−1	1.380−1	4.011−2	8.621−3	8.220−2	5.254−2	1.678−4	4.919−2	5.796−2	7.874−3	8.540−3	3.431−2	3.269−2	5.841−2
15	1.978−2	8.049−2	1.094−1	4.045−2	2.290−3	5.707−2	5.055−2	1.241−3	2.708−2	4.948−2	1.541−2	8.655−4	1.717−2	2.225−2	4.086−2
16	1.279−2	5.406−2	7.813−2	3.375−2	3.488−4	3.604−2	4.012−2	3.256−3	1.335−2	3.517−2	1.660−2	8.467−5	7.245−3	1.304−2	8.302−3
17	6.988−3	3.026−2	4.547−2	2.154−2	1.362−5	1.908−2	2.462−2	3.219−3	5.709−3	1.985−2	1.177−2	5.254−4	2.602−3	6.272−3	4.389−3
18	2.089−3	9.147−3	1.399−2	6.910−3	2.058−6	5.594−3	7.741−3	1.215−3	1.483−3	5.979−3	3.916−3	2.838−4	6.013−4	1.731−3	1.125−3
Σ	6.5719	5.6156	4.2402	3.2627	3.0544	2.8844	2.4409	2.1877	2.1398	1.9516	1.7461	1.6659	1.6143	1.5272	1.3969

900 Å, in steps of 50, to 450 Å are available from the authors. The maximum followed by the decaying oscillations of σ_{if} with v_f and the relatively smaller values exhibited for specific $v_i \rightarrow v_f$ combinations (such as $1 \rightarrow 3$, $3 \rightarrow 3$, $4 \rightarrow 2$, etc.) originate primarily from the behavior of the associated Franck-Condon factors.

Figure 3 displays the overall variation with initial vibrational level v_i and photon energy E (eV) of these individual cross sections summed over all accessible final discrete levels v_f. For $E \gtrsim 16.5$, corresponding to wavelengths λ shorter than 750 Å the photoionization is reduced, as v_i is increased from 0 through 14, by between a factor of 3 at 16.5 eV and a factor of ~5 at 30 eV (≡410 Å). Because of the smaller ionization thresholds the broad maxima of $\sigma_{if}(v_i)$ shift to lower E as v_i is increased. Each subsidiary jagged peak at low E reflects the vibrational edges resulting from a constant number of v_f becoming and remaining accessible over specified E ranges, a number which, of course, increases by unity as each successive vibrational threshold is passed.

In any experiment, however, the contribution arising from autoionization, presumably effective at these low E and not included in this present investigation, will swamp this vibrational pattern.

For photon energies E (eV) in the range 15.4 eV(≡804 Å) $\leq (E + E_{i_0}) \leq$ 18.1 eV(≡686 Å), where E_{i_0} is the energy of the initial v_i level of H_2 relative to $v_i = 0$, the residual ion is molecular, being left in the bound vibrational levels v_f(= 0–18) of H_2^+. More energetic photons can produce atomic H^+ ions formed indirectly via transitions to the continuum vibrational levels associated with the $1s\sigma_g$ electronic state of H_2^+, and directly via transitions to the repulsive $2p\sigma_u$ dissociative state. In the energy range 18.1 eV(≡686 Å) $\leq (E + E_{i_0}) \leq$ 29.1 eV(≡426 Å) dissociation into atomic ions originates from the former set of transitions, the importance of which can be assessed from the factor

$$C(v_i) = \left(\sum_{v_f=0}^{18} \left| \langle v_i(H_2) | v_f(H_2^+(1s\sigma_g)) \rangle \right|^2 \right)^{-1} - 1, \qquad (35)$$

which represents the (H^+/H_2^+) ratio of ion content. This factor is found to increase from 0.015 for $v_i = 0$ to 0.434 for $v_i = 7$ and then declines to 0.061 for $v_i = 14$. The present values for $C(v_i = 0\text{–}12)$ displayed in Table II are to within 0.002 of those of Ford and Docken[12] who however obtain 0.127 and 0.049 for $C(13)$ and $C(14)$ which are respectively 10% and 20% smaller than the present values. This difference may be due to the present use of the 1975 potential of Kolos and Wolniewicz[20] which is presumably a more accurate representation at larger R than the earlier ones used by Ford and Dock-

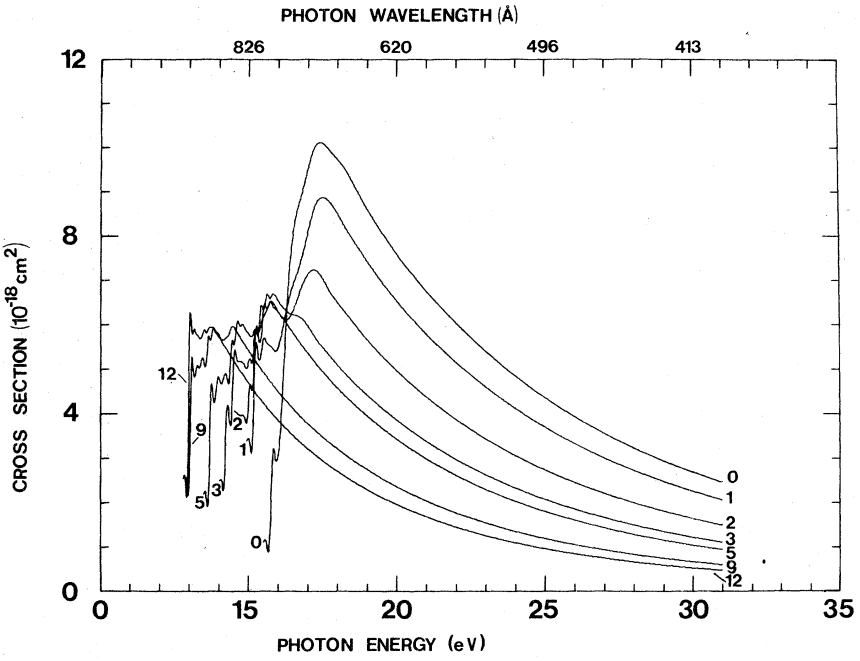

FIG. 3. Cross sections (10^{-18} cm^2) for the photoionization $h\nu + H_2(X\,^1\Sigma_g^+, v_i) \rightarrow H_2^+(X\,^2\Sigma_g^+, \sum_{f=0}^{18} v_f) + e$ as a function of photon energy. Values of v_i are as indicated.

en.[12] These important transitions can now be acknowledged directly by applying the closure relation to (7) so as to obtain

$$\sigma_{if}(\nu; v_i) = \sum_{v_f} \sigma_{if}(\nu; v_i, v_f)$$
$$= \tfrac{4}{3}\pi^2\, \alpha h\nu \left[4\langle v_i | M_x^2(\bar{\epsilon}, R) | v_i\rangle + \langle v_i | M_z^2(\bar{\epsilon}, R) | v_i\rangle\right] \qquad (36)$$

for the cross section for photoionization of $H_2(v_i)$ with formation of both atomic and molecular ions *by photons of sufficient energy to excite all the vibrational bound and continuum channels* associated with $H_2^+(1s\sigma_g)$. This cross section involves the selection of an average ejected energy $\bar{\epsilon}$ obtained from (4) by taking the transition energy to be the Franck-Condon average,

TABLE II. Cross sections (10^{-18} cm^2), Σ and S for ionization of $H_2(X\,^1\Sigma_g^+, v_i)$ by photons of wavelength λ with formation of molecular ions alone and of both atomic and molecular ions, respectively. The H^+/H_2^+ ion content ratio at 500 Å and associated frequency-independent plateau values $C(v_i)$ are also given.

λ		675 Å		600 Å		500 Å			
v_i	E_{fi} [a]	Σ	S	Σ	S	Σ	S	$(S/\Sigma - 1)$	$C(v_i)$
0	16.30	9.347	9.566	7.004	7.138	4.448	4.529	0.018	0.015
1	16.03	8.060	9.080	6.003	6.766	3.765	4.241	0.126	0.094
2	16.76	6.163	8.572	4.549	6.377	2.791	3.956	0.417	0.275
3	15.51	4.807	8.074	3.514	5.984	2.107	3.679	0.746	0.431
4	15.26	4.537	7.581	3.294	5.591	1.957	3.413	0.744	0.397
5	15.03	4.316	7.122	3.115	5.235	1.837	3.178	0.730	0.363
6	14.79	3.693	6.675	2.642	4.895	1.539	2.958	0.922	0.428
7	14.57	3.337	6.210	2.371	4.543	1.369	2.733	0.996	0.434
8	14.35	3.278	5.773	2.321	4.210	1.334	2.521	0.890	0.369
9	14.14	3.011	5.331	2.119	3.864	1.208	2.302	0.906	0.356
10	13.93	2.715	4.893	1.898	3.519	1.073	2.086	0.994	0.354
11	13.73	2.605	4.424	1.812	3.162	1.018	1.862	0.829	0.294
12	13.54	2.533	3.903	1.757	2.773	0.985	1.622	0.647	0.214
13	13.39	2.402	3.322	1.663	2.346	0.933	1.363	0.461	0.141
14	13.35	2.200	2.615	1.527	1.837	0.865	1.059	0.224	0.061

[a] Franck-Condon averaged transition energy (38).

$$\bar{E}_{fi} = \sum_{f=0}^{18} E_{fi} \left| \langle v_i(H_2) | v_f(H_2^+) \rangle \right|^2 + \int (\epsilon' + E_{i\infty}) \left| \langle v_i | v_{\epsilon'} \rangle \right|^2 d\epsilon', \quad (37)$$

where $E_{i\infty}$ is the dissociation energy of $H_2^+(1s\sigma_g)$ relative to the v_ith level of H_2 and where $|v_{\epsilon'}\rangle$ is the energy-normalized continuum vibrational function for the $(H^+\text{-}H)$ system dissociating with relative energy ϵ'. Application of closure to (37) yields,

$$\bar{E}_{fi} = \sum_{f=0}^{18} E_{fi} \left| \langle v_i | v_f \rangle \right|^2 + E_{i\infty} \left(1 - \sum_{f=0}^{18} \left| \langle v_i | v_f \rangle \right|^2 \right) + \int \epsilon' \left| \langle v_i | v_{\epsilon'} \rangle \right|^2 d\epsilon', \quad (38)$$

which can be evaluated directly from the present bound-bound Franck-Condon factors of Sec. II D, and from the ion kinetic energy distribution of Ford and Docken.[12] The averaged transition-energy (38) and associated photoionization cross sections (36) are presented in Table II at representative photon wavelengths, together, for comparison, with the cross sections arising from bound-bound vibrational transitions to the continuum are very important in the photoionization of vibrationally excited levels of H_2, particularly for those v_i in the 4–9 range when there are as many atomic ions H^+ produced as molecular ions H_2^+. For example, from Table II, the (H^+/H_2^+) ion content $(S-\Sigma)/\Sigma$ at 500 Å is 0.018, 0.996, and 0.224 for $v=0$, 7, and 14, respectively, to be compared with the corresponding frequency-independent values $C(v_i)$, thereby indicating the serious breakdown of the Franck-Condon approximation for photoionization of these excited vibrational states which involve larger R over which the electronic matrix elements are varying quite rapidly (cf. Figs. 1 and 2) and cannot be counted as fixed at a particular value for all v_f including the continuum (see also Sec. IV B below.)

Also it is worth noting from Table II, that, while the ion content in general rises with photon energy ranging from 18.4 to 25 eV, for $v_i \geq 2$, it is essentially constant at 0.126 for $v_i = 1$ and shows a decrease from 0.023 to 0.018 for the ionization from the $v_i = 0$ level in that energy range. Moreover, these $v_i = 0$ results do not agree as well with the measurements of Browning and Fryar[23] as does the single-center treatment of Ford *et al.*[7] (see their Fig. 3). This discrepancy may well be due to the present use of the closure relationship (36) which tends to overestimate the continuum contribution particularly at the lowest photon energy in Table II of 18.4 eV (≡ 675 Å) when compared with 18.1 eV, the threshold for transitions to the vibrational continuum. Also the single-center calculations were carried out for $J_i = 1$ rather than for $J_i = 0$ as adopted here.

B. Photoionization from the ground vibrational level

The only experimental data for photoionization of H_2 pertain only to the ground vibrational level. Accordingly, in Fig. 4 are displayed the present theoretical cross sections $\sigma_{if}(\nu; v_i = 0, \sum v_f)$ which are in close agreement with the measurements (×) of Cook and Metzer[24] and with the total absorption data (Δ) of Samson and Cairns.[25] The present results are somewhat lower than the previous values of Flannery and Öpik[3] for photoionization of $H_2(v_i = 0)$. This reduction has been attributed to the much more accurate present evaluation of the electronic transition matrix $\bar{M}_{if}(\epsilon, R)$ over a more closely spaced and larger range of (R, ϵ) parameters, and to the use of highly accurate vibrational wave functions.

Also shown in Fig. 4 are the "dipole-length" results of Kelly[9] who fixed the nuclei at $1.4a_0$, used the electronic function[26] of Coulson for H_2 [which, in contrast to the Weinbaum[15] function (8), ignores configuration interaction and hence correlation], and a single-center continuum function appropriate to the field of H_2^+ at $1.4a_0$. Also displayed in Fig. 4 are the calculations of Ford *et al.*[7] who, while using a 14-configuration representation of H_2, adopted a single-center Coulomb function of unit charge for the ejected electron. The figure illustrates the rather remarkable accuracy achieved by the simple single-center and fixed-nuclei models

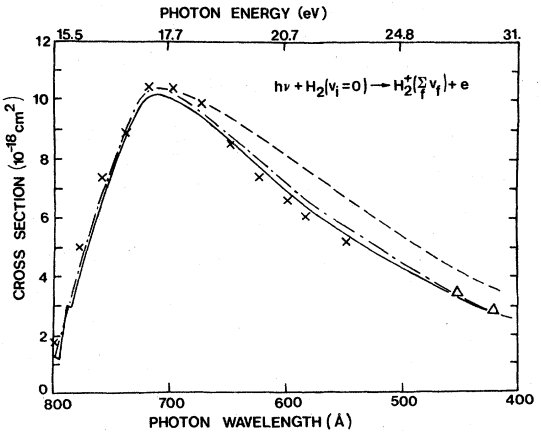

FIG. 4. Cross sections (10^{-18} cm^2) for the photoionization of $H_2(X\,^1\Sigma_g^+, v_i = 0)$ with formation of molecular ions in all vibrational levels. —: Present treatment; — — —: single-center approximation, Ford *et al.* (Ref. 7); – – –: single-center and fixed-nuclei approximation, Kelly (Ref. 9); ×: measurements of Cook and Metzger (Ref. 24); Δ: photoionization data of Samson and Cairns (Ref. 25).

TABLE III. Cross sections (10^{-18} cm^2) for photoionization of $H_2(v_i = 0)$ by 584-Å photons.

Theoretical		Experimental	
Present double-center treatment	6.57	Cook and Metzger[c]	6.3 ±15–20%
Single-center (Ford *et al.*)[a]	6.82	Bennett *et al.*[d]	6.51
Itikawa,[b] case (B)	6.43	Starr and Lowenstein[e]	6.19 ± 0.31
		Brolly *et al.*[f]	6.48 ± 0.17

[a] Reference 7.
[b] Reference 5.
[c] Reference 24.
[d] Reference 27.
[e] Reference 28.
[f] Reference 29.

for $v_i = 0$. Since the ingredients to the three theoretical basic models are not constant, no direct and full assessment of the single-center approximation is however possible, without resorting to further test calculations to be carried out below. In contrast to photoionization of the $v_i = 0$ level of H_2, the deficiencies in the single-center model become clearly apparent particularly for those higher vibrationally excited levels of H_2 which involve larger internuclear distances R where a one-center expansion becomes questionable and where the obvious lack of orthogonality between the one-center Coulomb orbital and the $1s\sigma_g$ orbital of H_2 involves increasing error.

For photon wavelengths λ from 804 Å(15.4 eV), the $v_f = 0$ threshold, to 686 Å(18.1 eV), the ion is left in the bound vibrational levels while for shorter wavelengths down to 425 Å, the H^+/H_2^+ ion ratio is of the order 2% (cf. Table II). The photoabsorption measurements of Samson and Cairns[25] shown in Fig. 4 therefore refer mainly to the H_2^+ residual ion and are in excellent agreement with the present results.

Table III displays the rather good agreement with more recent measurements[24-26] of photoionization of $H_2(v_i = 0)$ at 584 Å, the radiation emitted via the $(2^1P\text{-}1^1S)$ transition in helium. We also notice that the present result for $v_i = 0$ is 2% higher than a similar calculation of Itikawa.

IV. SIMPLIFYING APPROXIMATION

A. Single-center continuum wave functions

In an effort to assess the reliability, in general, of describing the ejected electron by a Coulomb function of charge unity centered at the midpoint of the nuclei, it becomes necessary to perform additional calculations since the electronic wave function for $H_2(1s\sigma_g^2)$ evaluated for the present two-center analysis differs from that used in the single-center treatment of Ford *et al.*[7] Accordingly, Table IV displays the desired comparison of the relevant dipole and overlap bound-free integrals in (20) and (21) evaluated by using the Weinbaum wave functions (8) for H_2 in the present two-center and one-center procedures. The latter task was accomplished with the aid of the computer program recently published by Docken and Ford.[30] The comparison shows that the single-center approximation, in general, underestimates the x component $d_g^e(\bar{x})$ of the bound-free dipole while overestimating the z component $d_g^e(\bar{z})$; the associated cross sec-

TABLE IV. Test of single-center approximation. One-electron dipole and overlap integrals given by the single-center (SC) and double-center (DC) treatments for zero ejected energy.

	$d_g^e(\bar{x})$		$d_g^e(\bar{z})$		$-S_u^e$	
R	SC	DC	SC	DC	SC	DC
0.6	1.157	1.155	1.722	1.738	0.402	0.404
1.0	1.329	1.332	2.103	2.090	0.652	0.672
1.4	1.441	1.466	2.442	2.299	0.874	0.887
1.4[a]	(0.509)	(0.565)	(0.888)	(0.732)	(0.527)	(0.491)
2.0	1.500	1.591	2.840	2.331	1.147	1.071
3.0	1.397	1.652	3.256	2.179	1.452	1.156
4.0	1.177	1.596	3.449	2.224	1.591	1.180
4.0[a]	(0.079)	(0.363)	(0.099)	(0.405)	(0.364)	(0.418)
5.0	0.922	1.500	3.360	2.389	1.555	1.179

[a] Values in parentheses pertain to energy of $\frac{1}{2}$ a.u. for ejected electron.

TABLE V. Single-center (SC) and double-center (DC) cross sections for photoionization of $H_2(v_i)$ by Lyman radiation of 912 Å as a function of v_i.

v_i	DC	SC
4	0.81	0.91
5	2.16	2.36
6	4.21	4.49
7	4.17	4.34
8	5.17	5.16
9	5.75	5.50
10	5.59	4.92
11	5.87	4.68
12	5.94	4.13
13	5.82	3.30
14	5.44	2.36

tions (7) are therefore less affected because of error cancellation. While the single-center procedure is, as expected, quite adequate for the smaller internuclear distances $R<2a_0$, it becomes quite unreliable for dipole integrals and overlaps involving larger R. As the energy of ejection ϵ is raised from zero, the magnitudes of the various integrals diminish while the percentage error associated with the single-center procedure rapidly rises, as indicated by the entries in Table IV for $\epsilon = 0.5$ a.u.

It is also worth noting that the present single-center results for $\vec{M}_{if}(R,\epsilon)$ do not depart appreciably from those tabulated by Ford *et al.*[7] who used a more elaborate electronic wave function (a 14-configuration valence bond description) for H_2. For example, at $R=1.4a_0$ and $\epsilon=0$, $M_x=1.702$ and $2^{1/2}M_z=1.540$ to be compared with the respective values 1.692 and 1.613 of Ford *et al.*[7]

The overall accuracy achieved by the single-center approximation is illustrated in Table V which compares the present two-center cross sections for photoionization of $H_2(v_i=4-14)$ by radiation of 912 Å, the Lyman limit, with the single center results of Ford *et al.*[11] The comparison in general is rather favorable, except for the higher $v_i \geq 10$ when errors as large as 57% are encountered. The observed agreement over the large range (4–9) of v_i can be reconciled with the conclusions associated with Table III when one remembers that the most probable value $\langle v_i|R|v_i\rangle$ of the internuclear distance R is, for $v_i=4-10$, in the range $1.4a_0-2.6a_0$, a range adequately described by the single-center treatment. For $v_i=11-14$, this averaged separation varies from $2.8a_0-5.2a_0$, a range over which the single-center approximation exhibits marked failure (cf. Table IV). Moreover, as noted earlier in Sec. III A, the present values of $C(v_i=13,14)$ do differ from those used in the single-center treatment and this difference therefore would partially contribute to the discrepancy shown in Table V for these levels.

In conclusion, the representation of an electron ejected from a homonuclear molecule by a Coulomb wave of charge unity centered at the nuclear midpoint provides reasonably accurate components of the bound-free dipole moment for small nuclear separations R. The model is more successful in predicting cross sections for photoionization of molecules in those vibrationally excited states with a mean nuclear separation $\langle v_i|R|v_i\rangle$ less than $\sim 2a_0$.

B. Fixed nuclei approximation

When there is no appreciable variation of $\vec{M}_{if}(R,\epsilon)$, the electronic matrix element (6), over a range of internuclear distances R considered important to the photoionization, then the cross section (7) reduces to

$$\sigma_{if}(\nu;v_i;v_f)=\tfrac{4}{3}\pi^2\alpha h\nu[4M_x^2(\bar{R},\epsilon)+M_z^2(\bar{R},\epsilon)] \times |\langle v_i|v_f\rangle|^2, \quad (39)$$

in which the matrix elements are evaluated at some fixed separation $\bar{R}$, usually taken as R_e, the equilibrium internuclear distance. The cross section for photoionization into all final vibrational levels v_f of H_2^+, including the continuum dissociative states is therefore

$$\sigma_{if}(\nu;v_i)=\tfrac{4}{3}\pi^2\alpha h\nu[4M_x^2(\bar{R},\bar{\epsilon})+M_z^2(\bar{R},\bar{\epsilon})], \quad (40)$$

where $\bar{\epsilon}$ is, in terms of some average energy $\bar{E}_{fi}$ of transition, given by

$$\bar{\epsilon}=h\nu-\bar{E}_{fi}. \quad (41)$$

When R_e is set equal to $\bar{R}$, then (40) is simply, with the aid of (33)

$$\sigma_{if}(\nu;v_i)=\tfrac{4}{3}\pi^2\alpha h\nu[4A_x^2(\bar{\epsilon})+A_z^2(\bar{\epsilon})]. \quad (42)$$

In this *fixed-nuclei* approximation, the variation of σ_{if} with v_i for a given photon energy $h\nu$ is therefore governed solely by the variation of the electronic matrix elements with ejected energy $\bar{\epsilon}$. Since the photoionization process is here regarded as a purely electronic "vertical" transition from level v_i at nuclear separation R_e, the following two choices for $\bar{E}_{fi}$ are possible: (a) the energy as measured vertically upwards from the point (v_i,R_e) of the potential energy curve of H_2 to the point of intersection $(v_f=2,R_e)$ with the H_2^+ potential-energy curve and (b) the average energy $\bar{E}_{fi}$ of transition as determined by the Franck-Condon mean (38). Both of these choices were explored and Table VI shows that these transition energies can be quite different, particularly for the higher $v_i \approx 3-14$. This difference is reflected in the associated cross sections columns (5) and (6) of Table VI. On comparison with the present two-center treatment (36)

TABLE VI. Test of fixed nuclei approximation with various mean transition energies $\bar{E}_{fi}$ and mean internuclear distances by comparison of cross sections (a)–(d) (10^{-18} cm^2) for photoionization of H_2 (v_i) at 600 Å.

v_i	$\bar{E}_{fi}$(a) (eV)	$\bar{E}_{fi}$(b) (eV)	$\langle v_i\|R\|v_i\rangle$ (a_0)	Fixed nuclei (a)	(b)	(c)	Full treatment (d)
0	15.95	16.30	1.449	6.521	6.878	7.791	7.138
1	15.44	16.03	1.545	6.020	6.595	6.885	6.766
2	14.95	16.76	1.646	5.581	6.330	6.564	6.377
3	14.49	15.51	1.752	5.197	6.089	6.226	5.984
4	14.06	15.26	1.864	4.865	5.860	5.863	5.591
5	13.66	15.03	1.983	4.577	5.648	5.483	5.235
6	13.29	14.79	2.112	4.328	5.446	5.079	4.895
7	12.94	14.57	2.254	4.113	5.259	4.657	4.543
8	12.63	14.35	2.413	3.927	5.086	4.215	4.210
9	12.34	14.14	2.596	3.769	4.920	3.923	3.864
10	12.09	13.93	2.816	3.637	4.767	3.530	3.519
11	11.87	13.73	3.091	3.528	4.625	3.125	3.162
12	11.70	13.54	3.464	3.442	4.498	2.690	2.773
13	11.57	13.39	4.037	3.379	4.399	2.192	2.346
14	11.49	13.35	5.219	3.343	4.368	1.648	1.837

[a]Approximation Eq. (40) of text with vertical transition energy $\bar{E}_{fi}$(a) and fixed equilibrium nuclear separation R_e for all v_i.
[b]Approximation Eq. (40) of text with Franck-Condon averaged transition energy $\bar{E}_{fi}$(b) and fixed R_e for all v_i.
[c]Approximation Eq. (40) of text with $\bar{E}_{fi}$(b) and mean nuclear separation $\langle v_i|R|v_i\rangle$ fixed for individual v_i.
[d]Full treatment, Eq. (36) of text, with $\bar{E}_{fi}$(b).

we see that, while procedure (b) does indeed introduce closer agreement for low v_i, it fails, quite markedly for the higher v_i. This failure arises directly by assigning, in (40), the equilibrium internuclear distance R_e for $\bar{R}$, a procedure which involves increasing error with increasing v_i and which is not essential to the basic approximation. Accordingly we have evaluated, for each vibrational level v_i, the vibrationally averaged separation $\langle v_i|R|v_i\rangle$ which, as indicated by column 4 of Table VI, indeed differs substantially from $R_e = 1.4a_0$ for all v_i except the low lying ones. Comparison between columns 7 and 8 of Table VI also illustrates the accuracy achieved by the fixed nuclei approximation (40) in which the above vibrationally averaged $\bar{R}$ and Franck-Condon averaged transition energies $\bar{E}_{fi}$(b) are used. Thus, in this version of the fixed nuclei approximation, the variation of σ_{if} with v_i for a given wavelength is controlled by the variation of both $\bar{E}_{fi}$ and $\bar{R}$ with v_i. This accuracy was obtained for all the wavelengths sufficiently short for photoionization to all discrete and continuum levels of the residual ion.

The attainment of this accuracy for the fixed-nuclei approximation required the evaluation of the electronic matrix $\vec{M}_{if}(R, \epsilon)$ over the range of $\langle v_i|R|v_i\rangle$ associated with all the initial excited levels v_i. Thus, part of the simplicity of the original method (42) which employed $\vec{M}_{if}(R_e, \epsilon)$ at one equilibrium nuclear separation R_e is lost. We have therefore shown that the fixed nuclei approximation is very reliable at shorter wavelengths when suitable averages are adopted for both $\bar{E}_{fi}$ and $\bar{R}$.

Finally, it is worth pointing out that the accuracy obtained by the original method (a) is largely fortuitous especially for the higher v_i [when the above modification (b) fails completely] since the error introduced by using a lower $\bar{E}_{fi}$(a), and hence higher $\bar{\epsilon}$, is partially offset by errors arising from the more serious assumption of fixing the nuclei at R_e for all v_i.

V. CONCLUSION

In summary, cross sections for photoionization of $H_2(^1\Sigma_g^+)$ in excited vibrational levels v_i have been obtained by a two-center treatment in which the electronic transition matrix element is averaged over the initial and final discrete vibrational levels of the molecule and product molecular ion respectively. The procedure yields very good agreement with the measurements for $v_i = 0$. As v_i is increased, substantial contributions to the photo-

ionization are found to originate from transitions to the vibrational continuum associated with the $1s\sigma_g$ state of H_2^+ with the consequent formation of H^+ atomic ions. We have also explored the inadequacies of both the single-center and the fixed-nuclei approximations and have concluded that the former model yields reasonably accurate cross sections for those vibrational states with a mean nuclear separation $\overline{R} \lesssim 2a_0$ while the latter approximation is indeed quite sensitive to the adopted values of both the separation of the fixed nuclei and of the transition energy.

---

*Research sponsored by U.S. ERDA under Contract No. E-(40-1)-5002-8.

[1]F. Wuilleumier and M. O. Krause, *Electron Spectroscopy*, edited by D. A. Shirley (North-Holland, Amsterdam, 1973), pp. 259–267 and references therein.
[2]P. G. Burke, in *Atomic Processes and Applications*, edited by P. G. Burke and B. L. Moiseiwitsch (North-Holland, Amsterdam, 1976), pp. 200–248 and references therein.
[3]M. R. Flannery and U. Öpik, Proc. Phys. Soc. Lond. 86, 491 (1965).
[4]G. B. Shaw and R. S. Berry, J. Chem. Phys. 56, 5808 (1972).
[5]Y. Itikawa, J. Electron Spectrosc. Relat. Phenom. 2, 125 (1975).
[6]S. P. Khare, Phys. Rev. 173, 43 (1968).
[7]A. L. Ford, K. K. Docken, and A. Dalgarno, Astrophys. J. 195, 819 (1975).
[8]F. Hirota, J. Electron Spectrosc. Relat. Phenom. 9, 149 (1976).
[9]H. P. Kelly, Chem. Phys. Lett. 20, 547 (1973).
[10]H. C. Tuckwell, J. Quant. Spectrosc. Radiat. Transfer 10, 653 (1970); J. Phys. B 3, 293 (1970).
[11]A. L. Ford, K. K. Docken, and A. Dalgarno, Astrophys. J. 200, 788 (1975).
[12]A. L. Ford and K. K. Docken, J. Chem. Phys. 62, 4955 (1975).
[13]A. Cohn, J. Chem. Phys. 57, 2456 (1972).
[14]A. Niehaus and M. W. Ruf, Chem. Phys. Lett. 11, 55 (1971).
[15]S. Weinbaum, J. Chem. Phys. 1, 593 (1933).
[16]M. R. Flannery, Proc. Phys. Soc. Lond. 85, 1318 (1965).
[17]D. R. Bates, K. Ledsham, and A. L. Stewart, Phil. Trans. R. Soc. Lond. A 246, 215 (1953).
[18]C. Flammer, *Spheroidal Wave Functions* (Stanford University, Stanford, Calif., 1957).
[19]T. F. Moran, M. R. Flannery, and D. L. Albritton, J. Chem. Phys. 62, 2869 (1975).
[20]W. Kolos and L. Wolniewicz, J. Mol. Spectrosc. 54, 303 (1975).
[21]G. Hunter, A. W. Yau, and H. O. Pritchard, At. Data Nucl. Data Tables 14, 11 (1974).
[22]J. W. Cooley, Math. Comput. 15, 363 (1961).
[23]R. Browning and J. Fryar, J. Phys. B 6, 364 (1974).
[24]G. R. Cook and P. H. Metzger, J. Opt. Soc. Am. 54, 968 (1964).
[25]J. A. R. Samson and R. B. Cairns, J. Opt. Soc. Am. 55, 1035 (1965).
[26]C. A. Coulson, Proc. Camb. Philos. Soc. 34, 204 (1938).
[27]S. W. Bennett, J. B. Tellinghuisen, and L. F. Phillips, J. Chem. Phys. 75, 719 (1971).
[28]W. L. Starr and M. Lowenstein, J. Geophys. Res. 77, 4790 (1972).
[29]J. E. Brolly, L. E. Porter, R. H. Sherman, J. K. Theobald, and J. C. Fong, J. Geophys. Res. 78, 1627 (1973).
[30]K. K. Docken and A. L. Ford, Comput. Phys. Commun. 11, 49 (1976).